Pis'ma v ZhETF, vol. 93, iss. 9, pp. 608 – 611

Kinetics of cell-to-cell spread of viruses

V. P. Zhdanov[1)]

Department of Applied Physics, Chalmers University of Technology, S-412 96 Göteborg, Sweden

Boreskov Institute of Catalysis RAS, 630090 Novosibirsk, Russia

Submitted 2 March 2011

Recent experiments indicate that many viruses can move between cells directly via the cell-cell contacts without diffusing through the extracellular environment. We present the first generic kinetic model describing intracellular viral kinetics in combination with this mode of spread of virions. Our Monte Carlo simulations show the specifics of the propagation of the infection front in this case.

Viral kinetics have long attracted attention of biochemists, biophysicists and mathematicians [1–4]. The general paradigm in this field is that virus infection occurs via binding of free virions to target cells followed by entry, replication, and release of new virions to the extracellular environment. The conventional kinetic models, focused on the extracellular aspects of this pathway, are either temporal or spatio-temporal and include ordinary differential equations or reaction-diffusion equations for the populations of healthy and infected cells and virions (see, e.g., Ref. [5] and references therein). There are also temporal models describing intracellular viral kinetics (see, e.g., Ref. [6] and references therein). A new avenue in this field is related to recent observations (reviewed in Ref. [7]) that many viruses, including HIV-1, herpes simplex virus and measles, can move between cells directly via the cell-cell contacts without diffusing through the extracellular environment (this new mode of viral dissemination may promote immune evasion). In this communication, we present the first generic kinetic model of intracellular viral kinetics with cell-to-cell spread of virions.

Diffusion is a very basic process. In the context of spread of viruses, as already noted, it can be described by using the reaction-diffusion equations. In the case of cell-to-cell spread of viruses, this approach is valid on the scale much larger than the cell size provided that the populations of virions in adjacent cells are nearly equal (these conditions allow one to operate with the gradients of concentration). The initial growth (just after infection) of the virion population in a cell is, however, well known to be exponential [8, 9], and this population can rapidly become large. For this reasons, the difference in the populations of virions in adjacent cells may often be appreciable, and accordingly the reaction-diffusion equations may fail. Taking this point into account, we use the Monte Carlo (MC) technique to simulate the kinetics under consideration. To specify our model, we first introduce the mean-field temporal kinetic equation describing virions in a cell and show how this equation can be converted to the reaction-diffusion equation. Then, we outline the algorithm of simulations of an array of cells and present the corresponding results.

Just after penetration of the first virion inside a cell, the main process is virion replication. On this stage, as already noted, the growth of the virion population is there exponential, i.e., the virion population in cell i (i specifies the cell location) can be described as $dN_i/dt = kN_i$, where k is the replication rate constant (this equation is of course coarse-grained, because in reality the replication occurs usually via a few steps; for our generic model, the coarse-grained description is sufficient). If the corresponding exponential growth of the virion population were unlimited, a cell would rapidly die. In reality, however, the growth of the virion population is usually limited and it may reach a steady state due to, e.g., the function of the intracellular antiviral defence system and/or limitation of the supply of species needed for the replication (see, e.g., Refs. [10, 11]), and the cell may live in an infected state. Focusing on this scenario, we consider that the replication rate is given by $W_r = kN_i/(1+\alpha N_i)$, where $(1+\alpha N_i)$ is the factor phenomenologically describing a decrease of the replication rate with increasing N_i or, more specifically, the transition from the first-order replication at $aN_i \ll 1$ to saturation at $aN_i \gg 1$ ($\alpha \ll 1$ is a dimensionless parameter). Taking also degradation and spread of virions into account, we have

$$\frac{dN_i}{dt} = \frac{kN_i}{1+\alpha N_i} - \kappa N_i - rN_i + \frac{r}{n}\sum_j N_j. \qquad (1)$$

The second term in this equation describes degradation of virions (κ is the degradation rate constant). The third term corresponds to the virion transitions from cell i to the nearest-neighbour (nn) cells (r is the transition rate

[1)] e-mail: zhdanov@chalmers.se

constant). The fourth term describes the reverse transitions (j marks the nn cells; n is the number of these cells).

If the populations of virions in adjacent cells are nearly equal, one can expand the terms describing migration of virions and convert Eq. (1) into the conventional reaction-diffusion equation,

$$\frac{\partial N}{\partial t} = D\Delta N + \frac{kN}{1+\alpha N} - \kappa N, \qquad (2)$$

where $D \equiv ra^2/n$ is the virion diffusion coefficient (a is the cell size).

Under steady-state conditions (with negligible or balanced migration), Eq. (1) (or (2)) predicts that the cells can be either in the healthy state with

$$N_i = 0 \qquad (3)$$

or in the stable infected steady state with

$$N_i = (k-\kappa)/\alpha\kappa. \qquad (4)$$

The latter state exists provided that

$$k > \kappa. \qquad (5)$$

The meaning of this condition is physically obvious.

After local initial infection, the transition to the stable infected steady state occurs via propagation of the infection front. In the framework of the conventional reaction-diffusion theory, the Fisher-Kolmogorov-Petrovsky-Piscounov expression for the front velocity is (see, e.g., Ref. [12] and references therein)

$$v \simeq 2(kD)^{1/2}. \qquad (6)$$

The MC simulations of the propagation of infection in an array of cells can be performed by using various algorithms. We employ the MC algorithm based on the introduction of the properly chosen rate, W_*, which is higher than the maximum total rate (i.e., the rate of all the possible processes) among the cells [13]. In our model, the viral replication, degradation and migration rates for each cell are $W_r = kN_i/(1+aN_i)$, $W_d = \kappa N_i$, and $W_m = rN_i$, respectively, and the total rate equals $W_r + W_d + W_m$. The simulations include sequential trials to realize one of these processes in one of the cells. For each trial, a cell is chosen at random, and a random number ρ ($0 \le \rho \le 1$) is generated. Replication or degradation is realized, i.e., N_i is incremented or decremented by one, if $\rho \le W_r/W_*$ and $W_r/W_* < \rho \le (W_r + W_d)/W_*$, respectively. Migration is performed, i.e., N_i is decremented by one and N_j in one of the randomly selected nn sites is incremented by one, if $(W_r + W_d)/W_* < \rho \le (W_r + W_d + W_m)/W_*$. If $\rho > (W_r + W_d + W_m)/W_*$, a trial ends without any event. After each trial, the time increment is $\Delta t = |\ln(\rho')|/(N_c W_*)$, where N_c is the number of cells, and ρ' ($0 < \rho' \le 1$) is a random number.

The simulations are run on a 2D $L \times L$ square lattice (in this case, $N_c = L^2$). Initially, one of the cells located in the center is assumed to be infected by a virion (for this cell, $N_i = 1$) while the other cells are considered to be healthy ($N_i = 0$). Formally, we use the no flux boundary conditions. During the MC runs shown below, the infection front did not reach, however, the boundaries. Thus, the type of the boundary conditions does not matter.

As already noticed (Eq. (5)), the propagation of infection is possible if the replication rate constant is larger that the degradation rate constant. Taking this condition into account, we use $\kappa/k = 0.1$ and $\alpha = 0.2$. With these parameters, Eq. (4) yields $N_i = 45$ for the infected steady state. For relatively fast virion migration, we use $r/k = 1$. To describe slow migration, we employ $r/k = 0.01$.

With the specification above, we have simulated spread of virions on a lattice with $L = 200$. The corresponding results are presented in Figs. 1–3. In particular, the average population of virions per cell, $\langle N_i \rangle = \sum_i N_i/N_c$, as a function of time is shown in Fig. 1 (note that the MC runs are performed up to reaching $\langle N_i \rangle = 10$). Typical spatial distribution of virions are exhibited in Figs. 2 and 3. For relatively fast virion migration (Figs. 2a and 3a), one can observe a narrow region where with increasing the distance from the center the virion population in cells drops from the value corresponding to the infected steady state (Eq. (4)) down

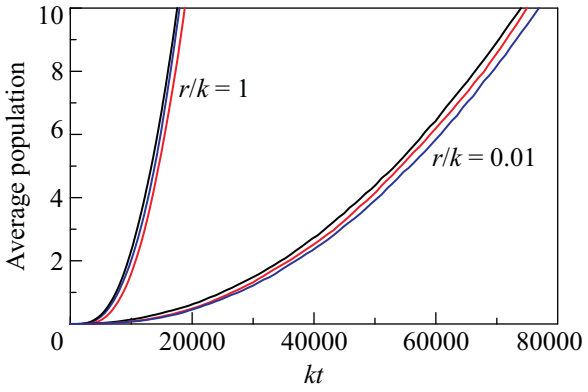

Fig. 1. Average virion population, $\langle N_i \rangle = \sum_i N_i/N_c$, as a function of time for $r/k = 1$ and 0.01. Each curve corresponds to a single MC run executed on a 200×200 lattice up to $\langle N_i \rangle = 10$

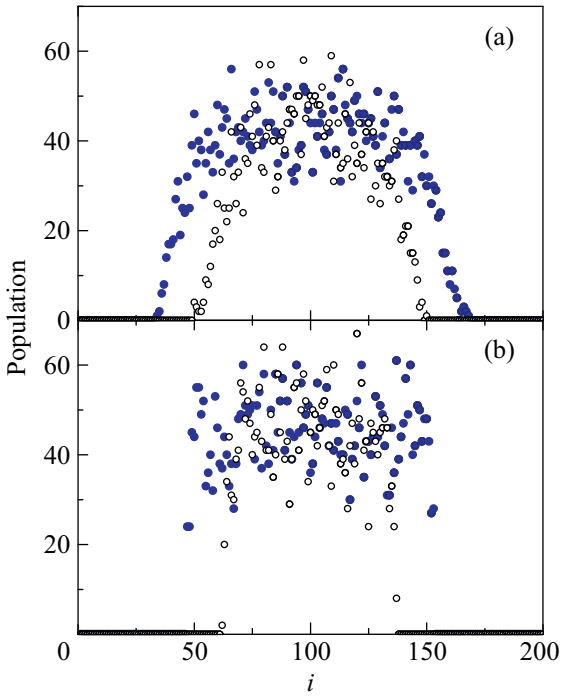

Fig. 2. Virion population, N_i, along a central horizontal row of cells during one of the MC runs (Fig. 1) with $r/k = 1$ (a) and 0.01 (b) at the moments when $\langle N_i \rangle = 5$ (open circles) and 10 (filled circles). The subscript i characterizes here the location of cells in a row and is used as the abscissa

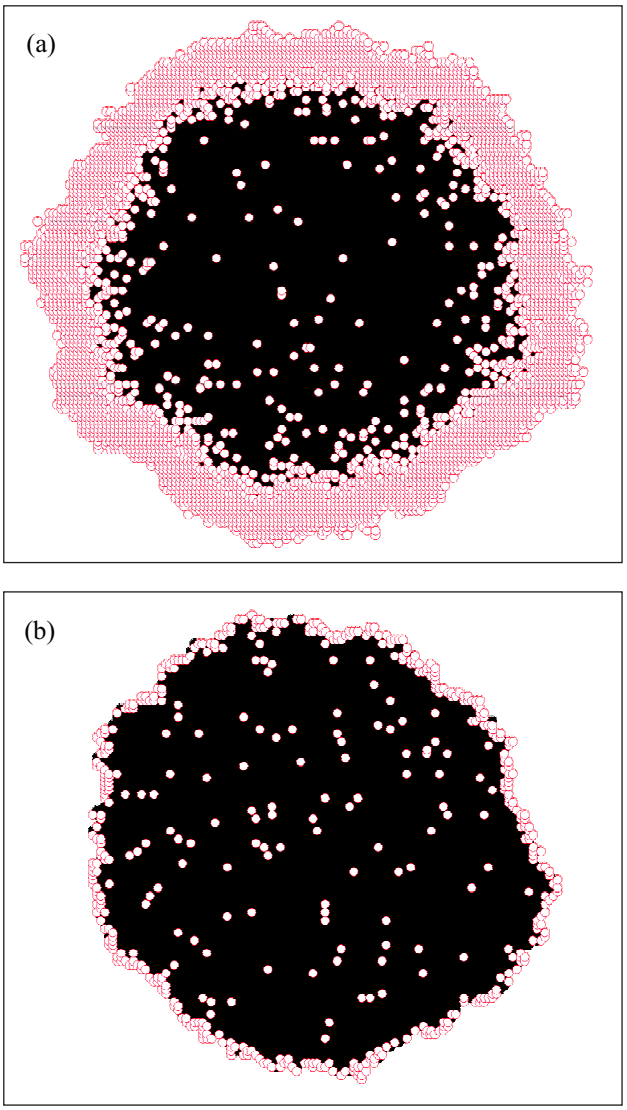

Fig. 3. Distribution of virions on the central 160×160 fragment of the 200×200 lattice in the end of one of the MC runs (Fig. 1) with $r/k = 1$ (a) and 0.01 (b). The cells with $N_i \geq 30$ are indicated by filled circles. The cells with $1 \leq N_i < 30$ are represented by open circles. The cells with $N_i = 0$ are not shown. Note that the filled circles overlap and form a black spot

to zero (Eq. (3)). For relatively slow migration (Figs. 2b and 3b), the thickness of this region becomes comparable with the cell size.

According to the conventional 2D reaction-diffusion theory, the radius of the infected area is vt, and accordingly the growth of the viral population should be of second order, $\langle N_i \rangle \propto \pi(vt)^2$. Our MC simulations (Fig. 1) indicate that the growth kinetics can approximately be fitted by using the the power law,

$$\langle N_i \rangle \propto t^{\beta}, \qquad (7)$$

where the growth exponent, β, is larger than 2. To scrutinize this aspect, we exhibit $\ln(\langle N_i \rangle)$ as a function of $\ln(kt)$ (Fig. 4). The slope of the curves obtained on a lattice with $L = 200$ shows that $\beta \simeq 2.4$ and 3.1 for relatively fast and slow virion migration, respectively. In the latter case, β is appreciably larger than 2. This is not surprising because in this case the sharp structure of the infection front (Figs. 2b and 3b) is far from conventional.

Looking at the curves obtained for $L = 200$ (Fig. 4), one can notice that the order of the growth slightly decreases with increasing time. Thus, one can expect that asymptotically (at $t \to \infty$) the front will reproduce itself and the growth exponent will be equal to 2. To increase time of the runs, we have increased L up to 500 and again performed simulations up to $\langle N_i \rangle = 10$. In this case, the slope of the curves (Fig. 4) indicates that $\beta \simeq 2.1$ and 2.7 for relatively fast and slow virion migration, respectively. Thus, the exponent for slow migration is still appreciably larger than 2 despite a large lattice size.

In summary, our generic model shows the specifics of the propagation of the infection front in the case of cell-

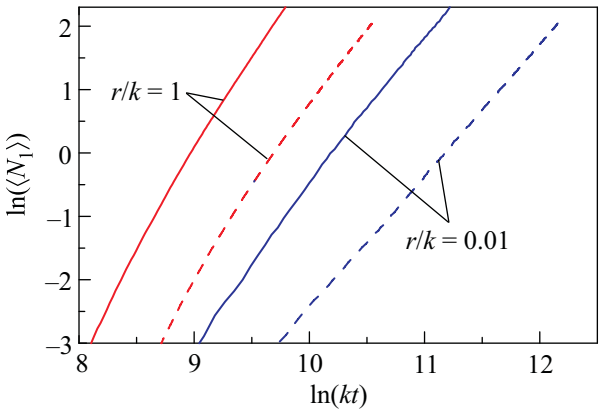

Fig. 4. Growth kinetics in the logarithmic coordinates for $L = 200$ (solid lines) and 500 (dashed lines). The kinetics for $L = 200$ represent two of those shown in Fig. 1

to-cell spread of virions. In a more general context, our MC simulations illustrate likely deviations in the propagation of the reaction fronts compared to the predictions of the conventional theory based on the reaction-diffusion equations (for the other aspects of this subject, see Ref. [12] and references therein).

Finally, we may articulate that the cell-to-cell mode of spread of virions has been firmly identified in several recent studies by using various measurements (reviewed in Ref. [7]). The corresponding temporal kinetics were, however, not tracked there in detail. The rate constants for various steps of the viral dynamics were not measured either. For these reasons, direct comparison of the results of our calculations with the experiment is now hardly possible.

1. G. I. Marchuk, *Mathematical Models in Immunology*, Springer, New York, 1983.
2. M. A. Nowak and R. M. May, *Virus dynamics. Mathematical Principles of Immunology and Virology*, Oxford University Press, Oxford, 2000.
3. A. S. Perelson, Nature. Rev. Immun. **2**, 28 (2002).
4. A. L. Bauer, C. A. A. Beauchemin, and A. S. Perelson, Inform. Sci. **179**, 1379 (2009).
5. R. Xu and Z. Ma, J. Theor. Biol. **257**, 499 (2009).
6. J. Sardanyes, R. V. Sole, and S. F. Elena, J. Virol. **83**, 12579 (2009); Y. Sidorenko, J. Schulze-Horsel, A. Voigt, U. Reichl, and A. Kienle, Chem. Eng. Sci. **63**, 157 (2008); E. L. Haseltine, J. B. Rawlings, and J. Yin, Comput. Chem. Eng. **29**, 675 (2005); V. P. Zhdanov, Phys. Biolog. **2**, 46 (2005).
7. Q. Sattentau, Nature Rev. Microbiol. **6**, 815 (2008).
8. P. Schuster, Theor. Biosci. **130**, 71 (2011).
9. V. P. Zhdanov, J. Phys. A: Math. Gen. **37**, L63 (2004).
10. K. Ozato, D. M. Shin, T. H. Chang, and H. C. Morse, Nature Rev. Immun. **8**, 849 (2008).
11. V. P. Zhdanov, Biosyst. **97**, 117 (2009).
12. O. Hallatschek and K. S. Korolev, Phys. Rev. Lett. **103**, 108103 (2009).
13. K. Binder, In: K. Binder (Ed.), *Monte Carlo Methods in Statistical Physics*, Springer, Berlin, 1979, pp. 1–45.